AAPS PharmSciTech, Vol. 10, No. 1, March 2009 (© 2009)
DOI: 10.1208/s12249-008-9167-0

Research Article

Polymeric Matrix System for Prolonged Delivery of Tramadol Hydrochloride, Part I: Physicochemical Evaluation

H. O. Ammar,[1,3] M. Ghorab,[2] S. A. El-Nahhas,[1] and R. Kamel[1]

Received 2 August 2008; accepted 21 November 2008; published online 9 January 2009

Abstract. Management of moderate or severe chronic pain conditions is the burden of clinicians dealing with patients trying to improve their quality of life and diminish their suffering. Although not a new opioid, tramadol has been recently rediscovered and widely used; this may be due to its favorable chronic safety and dependence profiles together with its high potency. Tramadol is a centrally acting analgesic with half-life of ~6 h; therefore, it requires frequent dosing. It is freely soluble in water; hence, judicious selection of retarding formulations is necessary. The current study is focused on the innovation of a novel, simple, monolayer, easy-to-use, cost-effective, and aesthetically acceptable bioadhesive transdermal delivery system overcoming the defects of the conventional "patch" as carrier system for tramadol, ensuring its adequate delivery, along with the physicochemical evaluation of the designed formulations. Monolithic tramadol matrix films of chitosan, different types of Eudragit®, and binary mixtures of both were prepared. As a single-polymer film, chitosan film showed best properties except for somewhat high moisture uptake capacity, insufficient strength and rapid release, and permeation. Polymer blends were monitored in order to optimize both properties and performance. Promising results were obtained, with chitosan–Eudragit® NE30D (1:1) film showing the most desirable combined, sufficiently rapid as well as prolonged release and permeation profiles along with satisfactory organoleptic and physicochemical properties.

KEY WORDS: matrix system; pain; polymers; tramadol hydrochloride.

INTRODUCTION

In the twenty-first century, pain has become the most common reason that patients seek medical attention, with chronic pain emerging as a major public health problem. Not surprisingly, individuals suffering from pain suffer as well from a significantly reduced quality of life (QOL) (1).

Opioids are the most powerful pain relievers, and therefore, traditional opioid analgesics remain the drug of choice for the medical treatment of severe acute pain syndromes and for progressive severe chronic illnesses. The most common side effects seen with opioid therapy are constipation, nausea, vomiting, sedation, itching, respiratory depression, tolerance, addiction, and physical dependence (2).

Tramadol is a synthetic, potent, atypical centrally acting analgesic with two distinct, opioid and non-opioid, mechanisms of action. The two enantiomers of racemic tramadol function in a complementary and synergistic manner to enhance its analgesic efficacy and improve its tolerability profile (3). In 1998, tramadol became the most widely used centrally acting analgesic worldwide; its success is a reflection of its favorable safety profile which differs significantly from other opioids (4).

Tramadol is rapidly absorbed after oral administration; the peak analgesic effect occurs 1 to 4 h after drug administration, with analgesia persisting for only 3–6 h. Tramadol is extensively metabolized in the liver where it undergoes biotransformation with the *O*-demethylated metabolite (M1) having ≈200 times higher affinity for μ-opioid receptors than the parent drug (4). It was therefore suggested that the *M1* metabolite may contribute to the analgesic effects of tramadol; however, delayed metabolism of tramadol may have a preferential advantage because it leads to delayed μ-opioid activity and consequently may reduce drug's abuse liability (5). Adverse effects and nausea, in particular, are dose-dependent, and therefore, the reduction of the amount of drug administered and the prevention of drug plasma peaks, while providing a simplified dosage regimen, are important factors for improving tolerability as well as patient confidence and QOL. Furthermore, a long-acting tramadol formulation may further enhance its overall efficacy and improve compliance by providing an around-the-clock analgesia and a more favorable safety profile (3).

Developing new opioids formulations with a decreased potential for diversion and abuse and increased efficiency

[1] Department of Pharmaceutical Technology, National Research Center, Dokki, Cairo, Egypt.
[2] Department of Pharmaceutics and Industrial Pharmacy, Faculty of Pharmacy, Cairo University, Cairo, Egypt.
[3] To whom correspondence should be addressed. (e-mail: husseinammar@hotmail.com)

continues to present challenges (6). Transdermal delivery (TD) is a new pharmaceutical approach which has been recently developed and is attaining great success. Historically, developments in TD have been incremental, focusing on overcoming problems associated with the barrier properties of the skin, reducing skin irritation rates, and improving the aesthetics associated with patch systems (7). As a molecule, based on its physicochemical properties (8), tramadol appears to be a suitable transdermal agent. Also, its pK_a is about 9.41; therefore, it is ionized and soluble over the pH range of interest.

Unfortunately, conventional TTS have some disadvantages which are related to their high cost as compared to other controlled release formulations, the less-than-ideal cosmetic appearance, and skin irritation, which present a major hurdle to patient acceptability (7).

In this study, we are concerned with a novel patch as a carrier for tramadol. We have tried to innovate a three-in-one 'soft' patch consisting of an elegant, aesthetically attractive, cost-effective, easy-to-handle monolayer polymeric film bioadhesive when applied to wet skin.

Tramadol HCl is freely soluble in water, and hence, judicious selection of release retarding formulations is necessary to achieve a constant drug input. Matrix system appears to be a very attractive approach in controlled release systems. The use of polymers has attracted considerable attention for the development of controlled release technology in the formulation of pharmaceutical matrix products (9). A prerequisite for progress in the design of novel drug delivery systems is the development of excipients that are capable of fulfilling multifunctional roles. Although a large number of synthetic and natural polymers are available for drug delivery applications, the use of novel combinations of polymers enlarge the scope of new drug delivery systems (10). Researchers have recently begun to study polymer–drug or polymer–polymer interactions in pharmaceutical formulations, considering them not as a detrimental occurrence but rather as a beneficial event that helps to control drug release (11).

In summary, in this study, we exploited polymeric matrix system technology in an attempt to deliver tramadol properly and safely *via* transdermal route in a trial to provide patients with a substantial pain relief, restoring their ability to work, improving their functional status and, consequently, their QOL. This part of the study comprised the physicochemical evaluation of the formulated polymeric films.

MATERIALS AND METHODS

Materials

Tramadol hydrochloride (T) was kindly provided by ADWIA Corp., Egypt; chitosan, highly viscous, Fluka, BioChemika, Japan; Eudragit® NE 30D, Eudragit® RS PO, and Eudragit® RL PO were generously donated by Rohm Pharma, Darmstadt, Germany; di-*n*-butylphtalate (DBP), Merck-Schuchardt, Germany; propylene glycol (PG), BDH Chemicals Ltd., England; triacetin (glyceryl triacetate), Sigma-Aldrich, Italy; polyethylene glycol 400 (PEG 400), s.d. fine-chem LTD, Mumbai, India. All other reagents were of pharmaceutical grade.

Methods

Preparation of Polymeric Monolithic Matrix Films

Preparation of Chitosan Monolithic Matrix Films. Chitosan 1% (*w*/*w*) was dispersed in 1% lactic acid solution at 70°C, then the drug and the plasticizer (40% *w*/*w* of polymer) were added with continuous stirring (using Velp Scientifica magnetic stirrer) to ensure uniform distribution (12). The films were then prepared by solvent evaporation technique.

Preparation of Eudragit® NE 30D Film. The 30% aqueous dispersion was diluted to reach a concentration of 10%, then the diluted dispersion was stirred with a magnetic stirrer for 2 h and allowed to stand for 30 min (13). The drug was added and the films were prepared as stated before.

Preparation of Eudragit® RL PO and Eudragit® RS PO Films. The polymeric solution (10% *w*/*v*) was prepared by dissolving Eudragit RL PO or Eudragit RS PO along with 40% plasticizer in isopropyl alcohol–dichloromethane (1:2) solvent system to obtain a clear solution (14). The drug was then added and the procedure was completed as previously stated.

Preparation of Mixed Polymeric Monolithic Matrix Films. Monolithic matrix films of chitosan with Eudragit® polymers (Eudragit® NE 30D, Eudragit® RL PO, Eudragit® RS PO) in a chitosan/polymer ratio 1:1 in formulations (E4, E5, E6) were prepared by dispersing chitosan in 1% lactic acid solution at 70°C. The second polymeric dispersion was added under continuous stirring, then the drug and plasticizer (40% *w*/*w* of total polymer weight) were added. The homogenous polymeric dispersion (1% *w*/*w*) was then poured in Teflon molds to prepare mixed monolithic films by solvent evaporation technique.

Physicochemical Evaluation of Prepared Polymeric Monolithic Matrix Films

Organoleptic Examination and Plasticizer Selection. Many physical and organoleptic characteristics including color, transparency, gloss, flexibility, elasticity, integrity, strength, smoothness, homogeneity, residue left on skin upon removal, security of location on skin (adhesion), and integrity on skin were examined in order to identify suitable formulations for the intended application and best plasticizer to be used with each polymer. The tested plasticizers comprised DBP, glycerin, polyethylene glycol 400 (PEG 400), triacetin, and PG. A simple rating score system was assigned to each criterion, with (+++) representing the most positive characteristics approaching or matching the target and (−−−) representing the most negative result.

Uniformity of Drug Content in the Films. A known weight of film was dissolved and diluted subsequently with distilled water, the solution was then filtered using 0.45 μm Millipore filter, and the concentration of tramadol hydrochloride was measured spectrophotometrically at 271 nm using Shimadzu UV Spectrophotometer (2401/PC), Japan (15) against a blank solution containing the same amount of polymer and plasticizer without drug (14).

Film Thickness. The thickness of prepared films was measured using a micrometer (Mitutoyo, Kanagawa, Japan) at three different places and mean values were calculated (14).

Moisture Uptake Study. The films were put in a desiccator with silica gel for 24 h and weighed (W_i) using Sartorius AG Göttingen electric balance, Germany. The films were then transferred to another dessicator containing saturated NaCl solution (relative humidity 75%) at 25°C until a constant weight was obtained. After equilibrium was attained, the films were taken out and weighed (W_m) (14,16). Moisture uptake capacity was calculated according to the following equation:

$$\text{Moisture uptake capacity } (\%) = (W_m - W_i/W_i) \times 100. \quad (1)$$

Moisture Content Study. The prepared films were weighed (W_i) and kept in a desiccator containing silica gel at 25°C until it showed a constant weight (W_d) (14,16). The moisture content was calculated according to the following equation:

$$\text{Moisture content } (\%) = (W_i - W_d/W_d) \times 100. \quad (2)$$

Swelling and Water Uptake Study. The water uptake was determined gravimetrically (17). The dried films fixed to stainless steel support were immersed in a beaker containing 25 ml distilled water at room temperature. At specific intervals up to 3 h, the swollen sample with the pre-weighed mesh were weighed after removal of excess surface water by light blotting with a filter paper. The experiment was discontinued when the film begin to disintegrate or dissolve. To quantify the swelling process, the swelling index percentage was calculated as follows:

$$\text{Swelling index}\% = (W_s - W_d/W_d) \times 100 \quad (3)$$

where W_d is the weight of the dried polymer film and W_s denotes the weight after swelling.

Mechanical Properties Study. The mechanical properties were evaluated using Chatillon® apparatus for force measurement (greensbro, NC 27409). Rectangular film strips of fixed width and length were fixed between the upper and lower jaws. The lower jaw was driven downward with a speed of 1 mm/s. Load *versus* displacement curves were recorded until rupture of the film (18). The mechanical properties were determined as follows:

$$\text{Tensile strength} = \text{Breaking force/area of the film} \quad (4)$$

$$\text{Elongation at break}\% = \text{Difference in length at breaking point} \times 100/\text{original length} \quad (5)$$

$$\text{Energy at break} = \text{AUC/V} \quad (6)$$

where AUC is the area under load *versus* displacement curves and *V* is the volume of the film located between upper and lower jaws (the energy at break is normalized to the film's volume).

pH Measurement. The pH of the film forming solutions was measured using 3510 Jenway pH meter, UK which was calibrated before use (19).

FTIR Study. The pure drug, the unmedicated monolithic matrix films (or the polymer), and the films containing the drugs were mixed separately with IR grade KBr in the ratio of 100:1, and corresponding discs were prepared by applying 5.5 metric tons of pressure in a hydraulic press. The discs were scanned over a wavenumber range of 4,000–400 cm^{-1}.

In vitro Release Studies Using USP Dissolution Tester. The dissolution studies were performed according to USP 23 apparatus 5 using dissolution test unit, Hanson Research Corp., USA (20); 1,000 ml of distilled water (12,15,20) was used as dissolution medium. The temperature was adjusted at 32±0.5°C and the speed at 50 rpm. Aliquots of 5 ml were withdrawn through sintered glass filter at each time interval and replaced by equivalent amounts of fresh dissolution media. Blank experiments were simultaneously performed. Decisive release parameters, percent cumulative amount of drug released after 5 h (% Q_5), release efficiency percentage (% RE), mean release time (MRT), estimated time to achieve 100% release (T_{100}), diffusion coefficient (D), were calculated to compare different formulae.

Ex vivo Permeation Studies. The skin permeation studies were performed using full-thickness naked abdominal rat skin. The skin was kept frozen until use within 1 week (21). Vertical type Franz diffusion cells (Vangard International Inc., USA) were used. Distilled water (22) containing 0.005% sodium azide as preservative (23) was used as receptor medium and was agitated at 300 rpm and 37±0.5°C. After equilibration of the skin with receptor phase, the barrier integrity was inspected visually. The medicated circular film of surface area 5 cm^2 was placed in the donor compartment. Parafilm® was used to occlude the donor and receptor chamber and prevent solvent evaporation. A similar set was run simultaneously using unmedicated patch at the donor compartment as a skin-patch control system to avoid the influence of inherent extracts from the skin or leaching of any material from the patch without drug (16). Samples of the receptor fluid (1 ml) were withdrawn at various time intervals up to 24 h and replaced immediately with fresh distilled water, then the samples were filtered and assayed spectrophotometrically at 271.

All statistical analyses were done according to the one-way analysis of variance test followed by the least significant difference procedure using the SPSS® software.

RESULTS AND DISCUSSION

Physicochemical evaluation and appropriate quality control are essential to ensure safety and adequate performance of designed formulae.

Table I. Organoleptic Properties of Monolayer Polymeric Matrix Films

Properties	Film						
	Chitosan	Eudragit NE	Eudragit RL	Eudragit RS	E4	E5	E6
Best plasticizer	Glycerin	–	PEG 400	PEG 400	Glycerin	Glycerin	Glycerin
Color	Faint yellow	Faint white	Yellowish white	Yellowish white	Faint white	Faint yellow	Faint yellow
Transparency	Transp.	Transp.	Opaque	Opaque	Transp.	Transp.	Transp.
Gloss	+++	+	+	+	+++	+++	+++
Flexibility	+++	++	+	+	+++	++	++
Elasticity	+++	++	++	++	+++	++	++
Integrity	+++	++	++	++	+++	+++	+++
Strength	+	++	++	++	+++	+++	+++
Smoothness	+++	+	+	+	+++	+++	+++
Homogeneity	+++	++	++	++	+++	+++	+++
Residue left on skin upon removal	+	+	+	+	+	+	+
Security of location on skin (adhesion)	+++	−	+	+	+++	++	++
Integrity on skin	+++	+	+	+	+++	+++	+++

Organoleptic Examination and Plasticizer Selection

The first and most important parameter for the development of a polymeric film is the choice of polymer. Besides having good film-forming properties and being a non-skin-irritant, the polymer must be soluble in a skin-tolerant solvent (24). The investigated polymers comprised natural polymer (chitosan) and synthetic polymers (Eudragit® NE 30D, Eudragit® RL PO, and Eudragit® RS PO). Apart from polymers, plasticizers exert a strong influence on the properties of formed films (25), resulting in higher flexibility, reduced brittleness, increased strength, improved adhesiveness of the film with other surfaces or membranes (26), and changed permeability of the films. For each polymeric film, 40% of five different plasticizers, DBP (lipophilic) and glycerin, PEG 400, triacetin and PG (hydrophilic), were examined to obtain the best suitable and aesthetically acceptable film properties for topical application allowing to attain targeted therapeutic effect and patient compliance.

For a first assessment of the suitability of the films from the patient's aesthetical point of view (24), a simple rating score system has been developed (Table I).

Most conventional transdermal patches contain an impermeable backing layer leading to occlusion and, consequently, increased risk of skin irritation and infection. The designed polymeric bioadhesive film has a monolayer structure which is supposed to avoid pronounced skin occlusion.

Chitosan has received great attention for medical and pharmaceutical applications due to its beneficial intrinsic properties (27). Chitosan is suited for repeated adhesion. Its adhesive properties result from the interaction between positive charges of chitosan and negative charges of skin. Chitosan has excellent film-forming properties as well as a potential for controlling drug release (28). In this study, lactic acid was used to solubilize chitosan. Some reports indicate that application of films prepared from chitosan–acetic solutions caused erythema and edema to rabbit skin, whereas films prepared from chitosan–lactic acid solution were non-irritant. Furthermore, lactic acid can improve the flexibility of the film because of its plasticizing action (29). It is also a highly effective moisturizer.

For chitosan monolithic matrix film (Table I), glycerin showed the best properties; the resultant film is almost ideal in characters except for the insufficient strength.

The use of Eudragits® for controlled drug delivery has been well known for several years (30). It is obvious that PEG 400 was the best plasticizer ameliorating the properties of RL and RS types. A previous study (13) has shown that by the addition of PEG, the polymeric network becomes less dense because of an increase in the mobility of the polymeric chains and in the free volume between the chains, causing the polymeric network to relax; therefore, the consequences of the plasticizing action of PEG are favorable to the properties of the films, while NE type formed strong, flexible and elastic film without the need of plasticizer. It was reported that Eudragit® NE 30D gives highly flexible films and has a low minimum film formation temperature (31). All Eudragit® films showed high strength, but poor skin adhesion and flexibility also, except NE type which were difficult to remove from the mold while keeping their integrity.

A great effort has been devoted to optimize the innovated films as far as possible. However, optimal properties cannot be achieved for a single polymer. Therefore, blending of polymers is necessary to attain more suitable transdermal devices (32) regarding properties and performance. Binary blends of chitosan and the different types of Eudragit® were done in a trial to ameliorate physicochemical properties and to optimize performance. Glycerin was the plasticizer forming mixed films of the best properties (Table I).

Uniformity of Drug Content

Homogeneous uniform drug distribution is one of the important characteristics of a transdermal patch that ensures the uniform reproducible sustained release of the drug from the patch (33). Estimation of drug content at different parts of the film indicated that the drug is uniformly distributed throughout the films (Table II), evidenced by the low values of the SD and coefficient of variation. This assures that the rheological properties of the casting solutions were suitable to ensure homogenous drug dispersion throughout the casting and drying process (34).

Table II. Drug Content Uniformity, Thickness Uniformity, Moisture Content, and Moisture Uptake Capacity of the Monolithic Matrix Films and pH of the Corresponding Film-Forming Solution

Film	Drug content %±SD	C.V. %	Film thickness (mm)± SD	C.V. %	% Moisture content± SD	% Moisture uptake ± SD	pH±SD
Chitosan	90.00±0.50	0.55	0.050±0.009	18.00	2.10±0.02	3.26±0.08	4.41±0.06
Eudragit® NE 30D	89.91±0.43	0.48	0.550±0.014	2.55	1.03±0.04[a]	0.73±0.07[a]	6.80±0.03
Eudragit® RL PO	94.92±0.51	0.54	0.500±0.019	3.80	1.82±0.02[a]	1.32±0.08[a]	4.20±0.03
Eudragit® RS PO	93.90±0.62	0.66	0.400±0.020	5.00	1.12±0.09[a]	0.99±0.15[a]	4.40±0.07
E4	91.99±0.09	0.10	0.070±0.007	10.00	1.60±0.04[b]	1.14±0.07[b]	5.80±0.06
E5	101.04±0.11	0.11	0.065±0.006	9.23	2.00±0.04[c]	1.75±0.07[c]	4.41±0.05
E6	102.21±0.49	0.48	0.063±0.009	14.29	1.92±0.09[d]	1.20±0.15[d]	4.43±0.06

Each value represents the mean of three experiments±SD
[a] Significant difference ($p<0.05$) compared to chitosan film
[b] Non-significant difference ($p>0.05$) compared to Eudragit® NE film
[c] Non-significant difference ($p>0.05$) compared to Eudragit® RL film
[d] Non-significant difference ($p>0.05$) compared to Eudragit® RS film

Film Thickness

The uniformity of film thickness was evidenced by the low values of the SD and coefficient of variation (Table II). The films were generally thin, therefore aesthetically satisfactory and more acceptable (34).

It is important here to denote that the results of determination of film thickness as well as drug content indicate that the process employed to prepare the films was suitable, reproducible, and capable of producing films with minimal variability.

Determination of Moisture Uptake Capacity

Table II shows the percent moisture uptake capacity of monolithic films. The moisture uptake of the films was generally low; this will help the films to remain stable and protect them from microbial contamination. Generally, the moisture uptake capacity of films increases with increasing hydrophilicity of the polymer or plasticizer and the amount of hydrophilic polymers as well. Within single polymeric films, chitosan showed the highest capacity; this may be due to its intrinsic more hygroscopic nature compared to Eudragits® in addition to the presence of glycerin, which can absorb moisture from environment because of its humectant properties, as film plasticizer. Also, the presence of lactic acid can play an important role.

Considering the Eudragits®, moisture uptake capacity was in the following order RL > RS > NE. These Eudragits® are acrylic and methacrylic acid esters with some hydrophilic properties due to the presence of quaternary ammonium groups where RL possesses a higher amount of such groups (35). The presence of PEG in RL and RS films renders them more hydrophilic, favoring more water absorbing into their films than NE film. PEG, and glycerin as well, are water-soluble, so they can easily penetrate the film structure since they have many hydroxyl groups on their skeleton. Another explanation is that with the addition of PEG 400 or glycerin, the network may become less dense because of an increase in the mobility of the polymeric chains and in the free volume between the chains, causing the polymer network to relax. The consequences of the plasticizing action are favorable to the adsorption and absorption of water molecules to the film (13). This pore former is an effective tool in increasing the film's permeability, which might be explained by an increase in film porosity. It was therefore expected that the moisture uptake capacity of the composite film will be in the following order E5 > E6 > E4.

Mixing of chitosan with Eudragits® has generally decreased the moisture uptake capacity, with the composite films showing a desirable low uptake capacity, E4 attaining the lowest. Statistical analysis is shown in Table II.

Determination of Moisture Content of Monolithic Films

Table II shows that increasing hydrophilic components forming the films was accompanied by an increase in moisture content. The moisture content was generally low, a desirable property which could help the formulation to maintain its stability, reduce brittleness during long-term storage, decrease susceptibility to microbial contamination, and reduce bulkiness, therefore facilitating handling. Generally, chitosan, may be due to its higher hydrophilicity together with the presence of glycerin as plasticizer, showed a higher moisture content than Eudragits®. The composite films had a moisture content which is more or less as low as the Eudragits®, with E4 showing the lowest. Statistical analysis is shown in Table II.

Swelling and Water Uptake Studies

The study of the hydration of polymers used in sustained-release applications has been an area of interest because it is believed that it affects drug release from controlled-release matrix (36). The consequence of water uptake could be the formation of empty spaces within the film matrix that could make its structure less resistant to mechanical stresses (37).

The results of swelling of single-polymer films are listed in Table III; all attained maximum swelling after 4 min of the beginning of the experiment. Chitosan film showed the highest water uptake capacity (MSI=709.69%±40.15); chitosan is a hydrophilic polymer, of which NH_2 and OH groups have the ability to interact with water molecules (38). Also, the swelling of chitosan may be favored by the presence of

Table III. Swelling of the Monolithic Matrix Films

Time (min)	% Swelling index						
	Chitosan film	Eudragit® NE 30D	Eudragit® RL PO	Eudragit® RS PO	E4	E5	E6
1	588.00±33.26	92.51±2.62	92.51±13.08	128.61±16.37	96.20±1.36	730.59±102.99	456.53±36.15
2	588.70±33.30	107.14±3.03	138.67±19.61	133.27±16.96	121.61±1.72	746.58±104.99	493.95±39.12
3	681.20±38.53	109.18±3.09	149.19±21.10	142.43±19.75	131.71±1.86	817.35±114.44	556.84±44.10
4	709.69±40.15	115.01±3.25[a]	260.76±36.88[a]	155.14±19.63[a]	150.13±2.12[b]	839.27±117.50[c]	604.01±47.84
5	700.69±39.64	110.04±3.11	181.06±25.61	154.22±15.85	110.52±1.56	653.42±91.48	660.61±52.32[d]
10	662.28±37.46	109.53±3.10	139.62±19.75	124.49±13.69	97.16±1.37	599.54±83.94	572.56±45.34
15	660.32±37.53	97.67±2.76	97.67±13.81	107.59±12.65	93.51±1.32	560.73±78.51	548.98±43.48
30	–	85.43±2.42	85.43±12.08	99.38±11.15	77.50±1.10	420.09±58.82	493.95±39.12
60	–	75.87±2.15	75.87±10.73	87.64±18.13	62.30±0.88	360.73±50.50	–
120	–	72.68±2.06	72.68±10.28	84.17±10.71	45.72±0.65	315.07±44.11	–
180	–	69.49±1.97	69.49±9.83	84.17±10.71	26.53±0.38	269.41±37.72	–

Each value represents the mean of three experiments±SD
[a] Significant difference ($p<0.01$) compared to chitosan
[b] Non-significant difference ($p>0.05$) compared to Eudragit® NE film
[c] Significant difference ($p<0.01$) compared to Eudragit® RL film
[d] Significant difference ($p<0.01$) compared to Eudragit® RS film

lactic acid used as solvent for chitosan and glycerin used as plasticizer (55). Visual observations indicated that chitosan matrix swelled greatly and has been highly expanded in size from the beginning; therefore, it begins to dissolve and fragment after 15 min.

Having more ammonium groups, the RL type showed more pronounced swelling (260.76%±36.88) than RS (155.14%±19.63) and NE (115.01%±3.25) types. The films maintain their integrity until end of the experiment, but RL film has expanded in size, whereas RS and NE films did not show such an expansion. The larger extent of water uptake of RL and RS compared to NE may be also due to the incorporation of PEG 400, a hydrophilic species, as plasticizer in RL and RS films.

The results of swelling of chitosan–Eudragit® composite films are shown in Table III. E4 and E5 films showed maximum swelling index after 4 min, while E6 showed maximum swelling index after 5 min and began to disintegrate after 30 min. As expected from previous results, E5 showed the highest degree of swelling (MSI=839.27%±117.50); this may be due to the hydrophilic nature of Eudragit® RL. Statistical analysis is shown in Table III.

Mechanical Properties Study

Mechanical properties are determined to characterize polymeric films for their abrasion resistance and elasticity or flexibility (24). Suitable films for intended application as transdermal drug delivery systems must be flexible enough to follow the movements of the skin without breaking, but at the same time, they must show an increased strength to prevent abrasion of the film caused for example by contact with clothing. Also, sufficient strength and flexibility is necessary so as not to crack or to be rubbed off during the wearing period and to be easily removed by peeling. Selection of the suitable plasticizer for the bioadhesive films has a profound influence on the mechanical properties (39).

Data presented in Table IV show that chitosan film exhibited excellent flexibility (percent elongation at break=220.00±21.78) and attained a markedly high energy at break (17.60±1.49 N/mm^2), but unfortunately, it was not strong enough (TS=0.008±0.000 N/mm^2) to withstand abrasion and rupture. Eudragit® films showed acceptable strength and acceptable elasticity, and NE film had the lowest strength (0.032±0.001 N/mm^2) but the greatest elasticity (percent elongation=200.00±19.80).

The binary blending of different polymers can have an obvious impact on the mechanical pattern of the resultant films. These phenomena might be attributed to the geometric packing of the polymer particles during film formation (18); in polymeric dispersions with bimodal size distributions, the ratio of volume of the small particles to the volume of the large particles strongly affects the extent to which interparticle voids are created during film formation. Mechanical properties can be improved by the improvement of polymer particles packing (with few voids). Chitosan–Eudragit® mixed films were almost ideal from the mechanical point of view. The films showed satisfactory strength, toughness, softness, and flexibility, with E4 film showing the most optimized properties. These results run in parallel with those previously reported by Wittaya-areekul *et al.* (27) concerning the inclusion of Eudragit® RS in chitosan films. Statistical analysis is shown in Table IV.

pH Measurement

For a dermatological preparation to be safe and nonirritant, its pH must be between 4 and 7 (40,57). The pH of the prepared film-forming polymeric solution was in the range of 4.2–6.8 (Table II), which is a desirable property.

FTIR Study

Interactions between drug and excipients play a vital role with respect to the physicochemical properties and performance of a certain formulation. In this study, Fourier transformation infrared spectroscopy (FTIR) techniques have

Table IV. Mechanical Properties of Monolithic Matrix Films

Film	Force (N)±SD	Tensile strength (N/mm^2)±SD	% Elongation at break±SD	Energy at break (N/mm^2)±SD
Chitosan	4.00±0.45	0.008±0.00	220.00±12.45	17.60±1.64
Eudragit® NE 30D	12.70±1.44	0.032±0.00[a]	200.00±11.31[b]	3.53±0.33[a]
Eudragit® RL PO	13.50±1.53	0.034±0.00[a]	187.50±10.61[b]	5.06±0.47[a]
Eudragit® RS PO	14.00±1.58	0.035±0.00[a]	180.00±10.18[b]	6.30±0.59[a]
E4 film	6.40±0.72	0.013±0.000[i]	200.00±11.31[f]	18.29±1.71[c]
E5 film	6.00±0.68	0.012±0.000[j]	190.00±10.75[g]	17.54±1.64[d]
E6 film	6.40±0.72	0.013±0.001[k]	184.00±10.41[h]	17.84±1.67[e]

Each value represents the mean of three experiments±SD
[a] Significant difference ($p<0.001$) compared to chitosan film
[b] Non-significant difference ($p>0.05$) compared to chitosan film
[c] Significant difference ($p<0.001$) compared to Eudragit NE film
[d] Significant difference ($p<0.001$) compared to Eudragit RL film
[e] Significant difference ($p<0.001$) compared to Eudragit RS film
[f] Non-significant difference ($p>0.05$) compared to Eudragit NE film
[g] Non-significant difference ($p>0.05$) compared to Eudragit RL film
[h] Non-significant difference ($p>0.05$) compared to Eudragit RS film
[i] Significant difference ($p<0.05$) compared to Eudragit NE film
[j] Significant difference ($p<0.05$) compared to Eudragit RL film
[k] Significant difference ($p<0.05$) compared to Eudragit RS film

been used to investigate any physical and chemical interaction (41) between the drug and the polymers used (Figs. 1 and 2).

Figure 1a shows the IR spectrum of tramadol hydrochloride. The principal well-defined peaks appeared at 3,306.20 cm^{-1} for the OH group, 3,062.68 cm^{-1} for the =CH of the aromatic ring, and 2,929.46 cm^{-1} for the –CH stretching. An obvious characteristic fingerprint appeared in the region 1,500–400 cm^{-1}.

The IR spectrum of chitosan (Fig. 1b) shows an absorption spectrum at 1,650.38 cm^{-1} assigned to the NH_2 of amide group and another at 1,736.68 cm^{-1} due to stretching vibration of C=O of the amide group. At 3,397.71 cm^{-1}, there appears a broad peak caused by O–H and N–H symmetrical vibration. The peak noticed at 2,940.42 cm^{-1} is assigned to C–H stretching. Peaks at the 1,200- to 1,000-cm^{-1} region are assigned to polysaccharide structure. In the case of the medicated film (Fig. 1c), an absorption band appeared at 3,380.31 cm^{-1} and another at 1,598.93 cm^{-1}; this shift may be due to H bonding between T and chitosan. Another peak appeared at 2,940.42 cm^{-1} attributed to C–H vibrational stretching. Also, an absorption band due to C=O appeared at 1,737.50 cm^{-1}.

Figure 1d shows the IR spectrum of Eudragit® NE30D film. The absorption band of the carbonyl group appeared at 1,739.78 cm^{-1}, while that of CH group at 2,924.80 cm^{-1}. While in the spectrum of the medicated film (Fig. 1e) the absorption band of O–H group of T appeared shifted to 3,441.32 cm^{-1} as a consequence of formation of H bonds with carbonyl group of Eudragit, this also can be the cause of the morphological change of C=O band appearing at 1,740.64 cm^{-1}.

Figure 1f, g shows the IR spectrum of Eudragit® RLPO and the medicated film, respectively. The C=O stretching absorption band appeared at 1,731.74 and 1,729.84 cm^{-1} in the case of the former and the latter, respectively, while the C–H stretching appeared at 2,951.22 and 2,947.72 cm^{-1}, respectively. The O–H stretching of T shifted to 3,406.66 cm^{-1} as a result of the hydrogen bonding taking place between the ester group of the polymer and the hydroxyl group of the drug.

Figure 1h shows the IR spectrum of Eudragit® RSPO polymer; the absorption band of carbonyl group stretching appeared at 1,730.97 cm^{-1} and the C–H stretching appeared at 2,952.88 cm^{-1}. The spectrum of the medicated film (Fig. 1i) showed a broad band at 3,391.03 cm^{-1} assigned to O–H stretching of T; the C=O stretching band was noticed at 1,740.73 cm^{-1}. The displacement occurring in these peaks may originate from the hydrogen bonding taking place between C=O of the ester group of the polymer and the hydroxyl group of the drug. Also, C–H stretching band appeared at 2,875.62 cm^{-1}.

Figure 2b, c shows the IR spectrum of mixed chitosan–NE unmedicated and medicated films, respectively. In the spectrum of the former, the broad peak caused by O–H and N–H symmetrical vibration in the molecule of chitosan shifted from 3,397.71 to 3,431.99 cm^{-1}; this may be due to the H bonds formation with the ester group of Eudragit®. The vibrational band of NH_2 of amide group of chitosan was noticed at 1,626.06 cm^{-1} shifted from 1,650.38 cm^{-1}, and the stretching band of C=O group appeared at 1,736.39 cm^{-1}. This displacement may confirm the hydrogen bonding with NE molecules. In the spectrum of E4 medicated film, the morphological as well as the positional change (from 3,431.99 to 3,346.74 cm^{-1}) in the broad peak assigned to O–H and N–H vibration may indicate a disruption of the some of the intermolecular interactions between the chains of the two polymers and the formation of new bonds with T molecules. This hypothesis is also supported by similar changes taking place in the band assigned to NH_2 of amide group which appeared at 1,581.85 cm^{-1} shifted from 1,626.09 cm^{-1}, in addition to similar change occurring to the C=O stretching band which appeared at 1,724.61 shifted from 1,736.39 cm^{-1}. All these statements may confirm T polymer(s) linking.

Figure 2d, e shows the IR spectrum of mixed chitosan–RL unmedicated and medicated films, respectively. The broad peak assigned to O–H and N–H vibration appeared at 3,426.05 cm^{-1} shifted from 3,397.71 cm^{-1}. This may prove the breakage of intra-polymeric link between chitosan chains and the formation of new chitosan–RL inter-polymeric association precisely between the COO groups of Eudragit and NH_2 (and/or OH) groups of chitosan molecules. As well, the vibrational bands of NH_2 of amide and C=O groups attributed a change in shape and position; the bands appeared

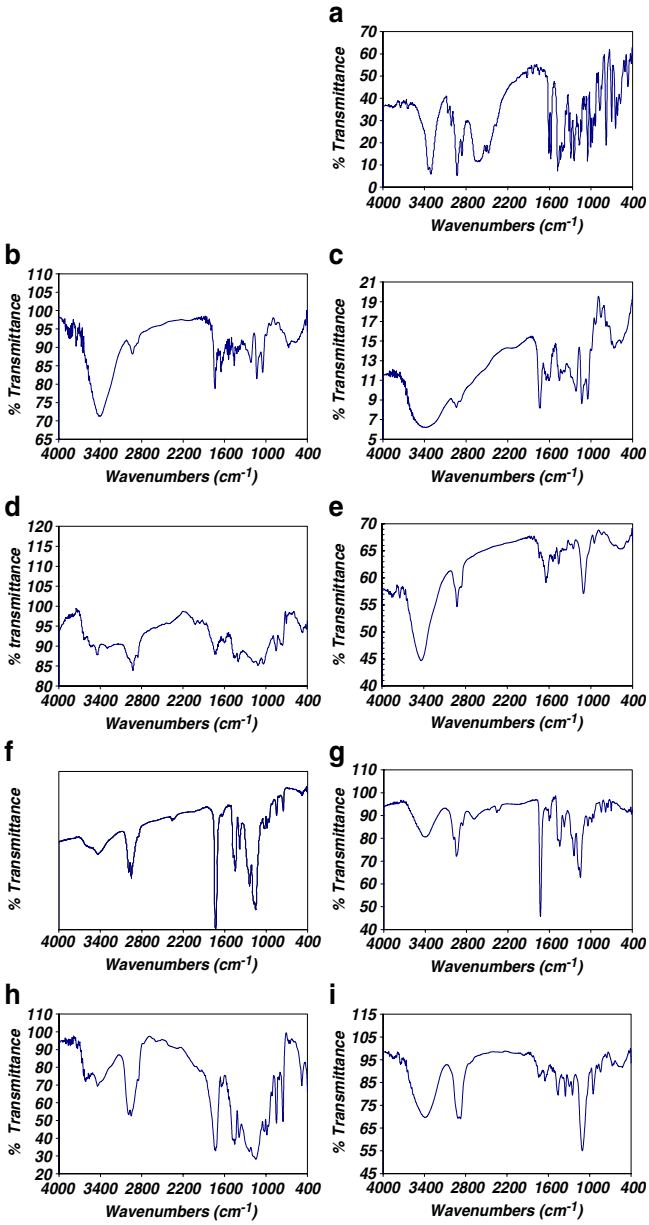

Fig. 1. FTIR spectrum of (**a**) Tramadol HCL, (**b**) chitosan polymer, and (**c**) medicated chitosan film, (**d**) NE film, (**e**) medicated NE film, (**f**) RL polymer, (**g**) medicated RL film, (**h**) RS polymer and (**i**) medicated RS film

at 1,620.85 and 1,738.69 cm^{-1}, respectively. Similar changes were noticed for the vibrational bands of the considered groups in the IR spectrum of the medicated film; this may evidence the hydrogen bonding between T and chitosan–RL polymeric network. The O–H and N–H vibration band appeared shifted to 3,431.20 cm^{-1}, and the stretching bands of NH_2 and C=O of amide groups were shifted to 1,603.36 and 1,735.85 cm^{-1}, respectively.

Figure 2f, g shows the IR spectrum of mixed chitosan–RS unmedicated and medicated films, respectively. As reported previously, the IR spectrum of E6 unmedicated film is showing band changes which may confirm polymer–polymer interactions. The O–H and N–H groups of chitosan showed the stretching vibrational band shifted to 3,426.16 cm^{-1}, while the peaks shifted to 1,744.78 and 1,624.25 cm^{-1} were assigned to the carbonyl and amino functions, respectively. The IR spectrum of medicated E6 film followed the same trend of other chitosan–Eudragit mixed films and showed spectrum changes suggesting drug–polymers interactions. The most interesting bands were noticed at 3,422.69, 1,737.52, and 1,646.14 cm^{-1} and showed both positional and morphological changes when compared to their corresponding bands in the IR spectrum of the unmedicated film. Considering the greater wavenumber shift noticed in the two latter bands, it is suggested that most drug–polymers interactions occurred with the amide function of chitosan and the ester function of Eudragit more than with the OH and NH_2 groups of glucosamine; this may be due to a certain molecular arrangement and physical entanglement of the polymeric chains within the formed IPN.

It can be concluded that changes noticed in the spectra in the range of 1,400–3,500 cm^{-1} indicated the polymer–polymer or drug–polymer(s) interactions which varied from weak to high intensity along the different polymeric systems under investigation.

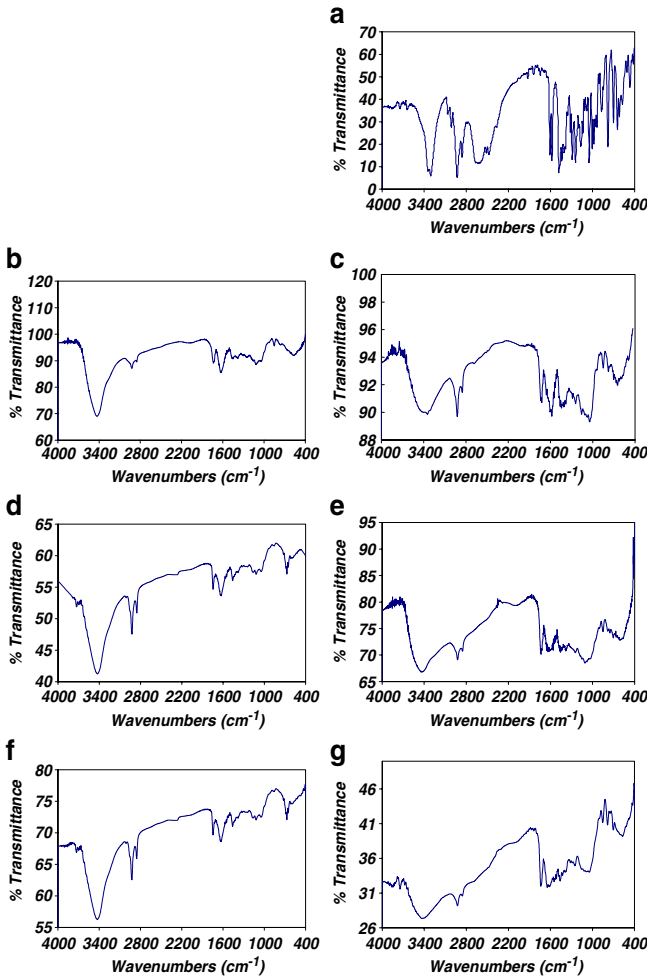

Fig. 2. FTIR spectrum of (**a**) Tramadol HCL, (**b**) E4 film, (**c**) medicated E4 film, (**d**) E5 film, (**e**) medicated E5 film, (**f**) E6 film and (**g**) medicated E6 film

In vitro Release Studies

The assessment of the release properties of TDS represents an important test for its pharmaceutical performance (42). The release experiment was carried out according to the FDA method (43). The cumulative amount of drug released was plotted *versus* time (Fig. 3) and release parameters were computed; these comprise:

- Cumulative drug amount released at 5 hours % (% Q5)
- Release efficiency (RE) (44)
- Mean release time (MRT) (45)

The MRT is a measure of the release or dissolution rate; the higher the MRT, the slower is the release rate.

- T_{100} dissolution time (T_{100}) (46)

It is the expected time to achieve 100 % drug release and was calculated using linear regression analysis.

- Diffusion coefficient (D) (47)

The MRT and RE are model-independent approaches which allow the translation of the profiles differences into a single value (47).

The kinetics of tramadol release was determined by finding the best fit of the dissolution data (drug-released fraction *versus* time) to distinct models: zero-order, first-order, and Higuchi. Furthermore, the Korsmeyer–Peppas semi-empirical model was applied (48,49):

$$Q_t/Q\infty = K_t^n \tag{7}$$

where $Q_t/Q\infty$ is the fraction of drug released at time t; k a characteristic constant comprising the structural and geometric characteristics of the dosage form, and n the release exponent, a parameter which depends on the release mechanism and is thus used to characterize it. This model is generally used to analyze the release when its mechanism is not well known or when more than one type of release phenomena are involved (50).

The initially rapid drug release from chitosan film reflected in the values of MRT, RE %, and T_{100} (Table V) may be explained by the rapid dissolution of the drug particles on the external surface of the device together with the cationic nature of both the drug and the polymer which can stimulate the fast diffusion of the drug out of the polymeric matrix, then the following slowing down of the release may be attributed to the decrease of T amount in the device and its slow diffusion through the polymeric matrix which become highly swelled a few minutes after the contact with the dissolution medium. Some previous studies have reported that the capacity of the polymer to swell is inversely related to release rate due to increasing the diffusional path length for drug molecules by swellable polymers (51). The release kinetics of chitosan film was not calculated because of the burst effect and fast release of the drug.

Considering the release parameters of Eudragit® matrix unilaminated films (Table V), RL type showed the fastest release compared to RS and NE types. This is explained by the more hydrophilic properties of RL regarding the presence of more ammonium groups in its structure (35), as previously explained in swelling experiments, in addition to the large cavity size in RL polymeric network. This can allow faster mode drug diffusion and may account for the higher permeability of RL type (31,52). Also, the repulsion between the cationic ammonium groups of RL or RS and that of T can have an accelerating effect on drug release from the polymeric matrix. All Eudragit® types followed square root of time law (Higuchi) kinetics (Table VI) where the main mechanism of drug release is Fickian diffusion, which is the predominating mechanism in case of water-insoluble polymeric systems, and the rate of drug release was found to be 0.2385, 1.3030, and 0.6053 mg/min$^{1/2}$ for NE, RL and RS, respectively (Table VI). In the case of RL film, Korsmeyer–

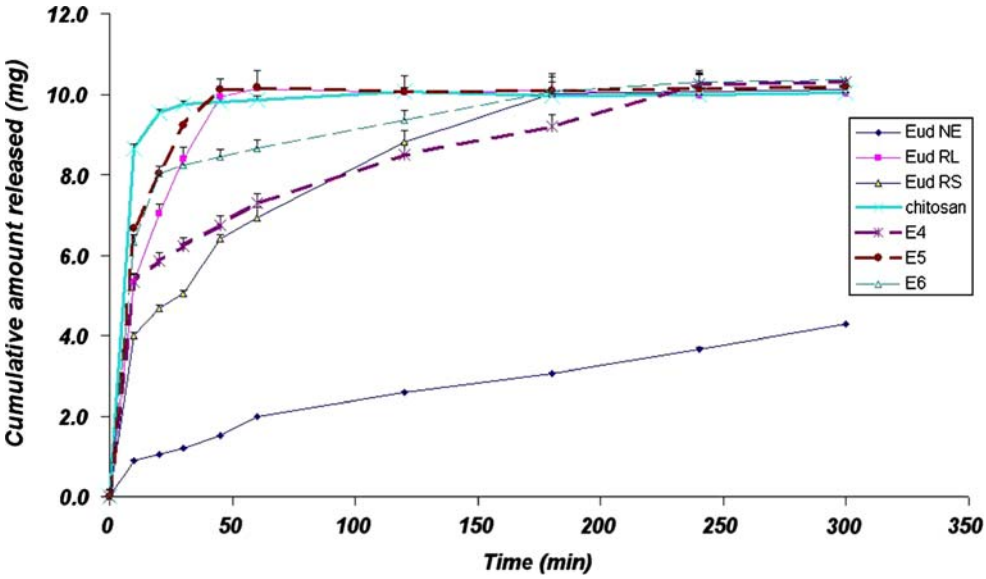

Fig. 3. Release profiles of tramadol HCl from monolithic matrix films

Table V. Release of Tramadol HCL from the Monolithic Matrix Films

Time (min)	Cumulative amount released (mg)±SD						
	NE 30D	RL PO	RS PO	Chitosan	E4	E5	E6
10	0.90±0.00	5.33±0.15	4.00±0.06	8.67±0.07	5.33±0.16	6.67±0.08	6.33±0.19
20	1.06±0.00	7.03±0.20	4.69±0.07	9.54±0.08	5.86±0.17	8.03±0.10	8.03±0.17
30	1.21±0.00	8.40±0.24	5.04±0.07	9.76±0.08	6.22±0.19	9.24±0.12	8.24±0.17
45	1.52±0.00	9.94±0.28	6.40±0.09	9.81±0.08	6.75±0.22	10.12±0.16	8.45±0.19
60	1.98±0.01	10.15±0.43	6.93±0.10	9.85±0.08	7.29±0.22	10.17±0.16	8.65±0.18
120	2.59±0.01	10.04±0.43	8.80±0.25	10.07±0.11	8.49±0.25	10.05±0.16	9.36±0.20
180	3.05±0.02	10.09±0.43	10.01±0.30	9.95±0.11	9.20±0.29	10.10±0.23	10.08±0.24
240	3.67±0.05	9.97±0.42	10.06±0.43	10.00±0.11	10.24±0.30	10.15±0.30	10.29±0.22
300	4.29±0.06	10.02±0.57	10.11±0.43	10.05±0.11	10.29±0.35	10.20±0.21	10.34±0.22
% Q_5±SD	42.88±0.55[a]	100.16±5.67[b]	101.09±4.29[b]	100.48±1.14	102.93±3.49[e]	102.00±2.14[f]	103.42±2.17[g]
% RE±SD	27.28± 0.23[a]	95.68± 4.17[b]	84.72±1.76[c]	97.47±1.03	85.86±3.26[h]	97.33±2.06[i]	93.06±2.06[j]
MRT±SD (min)	109.10± 0.81[a]	13.43±4.17[b]	48.59±2.91[d]	9.07±0.23	52.36±0.81[h]	13.73±2.43[i]	30.03±0.28[j]
T_{100} (min)	1756.68[a]	45.44[c]	171.95[d]	99.14	241.98[h]	41.64[i]	171.52[g]
Diffusion coefficient (cm^2/min)	1.78×10^{-5}	5.32×10^{-4}	1.15×10^{-4}	–	4.24×10^{-5}	3.08×10^{-4}	1.59×10^{-5}

Each value represents the mean±SD (n=3)
[a] Significant difference (p<0.001) compared to chitosan film
[b] Non-significant difference (p>0.05) compared to chitosan
[c] Significant difference (p<0.05) compared to chitosan film
[d] Significant difference (p<0.01) compared to chitosan film
[e] Significant difference (p<0.001) compared to NE film
[f] Non-significant difference (p>0.05) compared to RL film
[g] Non-significant difference (p>0.05) compared to RS film
[h] Significant difference (p<0.001) compared to NE
[i] Non-significant difference (p>0.05) compared to RL film
[j] Significant difference (p<0.05) compared to RS

Peppas equation was not applicable due to the fast drug release, while in the case of NE type, the value of n (0.4771) assures the diffusion-dependent release of tramadol. Such Higuchi kinetics has been already shown for some other drugs released from Eudragit® patches (52).

The release from NE film was too slow, and the expected calculated time for complete drug release was enormous (1,756.68 min.) compared to RL and RS types. In addition to the least hydrophilic properties and permeability of NE compared to RL and RS types (31), and of course chitosan, its larger thickness and the absence of plasticizer may be other factors contributing to it. Previous studies have shown that the thinner the matrix thickness, the faster was the release (39). Owing to the hydrophobic properties of NE compared to RL and RS, water could not deeply and freely penetrate the patch, so only the fraction of the drug near the external surface can be easily released to the dissolution medium (53). Also, PEG 400 was incorporated in RL and RS films, but not NE film (according to Rohm Pharma specification) which has the ability to form good films without the need of plasticizer. The softening of the polymeric matrix by the plasticizer can have an impact on drug release. Leaching of PEG from the films to the dissolution medium may lead to the formation of small pores facilitating drug release (39). Some studies are undertaken to improve drug permeability through formation of pores using hydrophilic additives. Hydrophilic additives increase the permeability of hydrophobic films by several mechanisms. For example, polyethylene glycol can erode and dissolve in the release medium and thus create pores in the film (13).

Polymethacrylates can be used as antinucleating agents which can interact with the active ingredient and effectively

Table VI. Release Kinetics of Tramadol HCL from Monolithic Matrix Films

Formula	Zero order		Higuchi order		First order		Korsmeyer–Peppas		
	Rate	R^2	Rate	R^2	Rate	R^2	K	n	R^2
NE 30D	0.0124	0.9388	0.2385	0.9938	0.0022	0.8940	0.0265	0.4771	0.9837
RL PO	0.1304	0.9858	1.3030	0.9998	0.0076	0.9552	–	–	–
RS PO	0.0349	0.9464	0.6053	0.9908	0.0022	0.8800	0.1980	0.2940	0.9200
Chitosan	–	–	–	–	–	–	–	–	–
Ch-NE 30D (E4)	0.0172	0.9378	0.3678	0.9902	0.0010	0.8975	0.3710	0.1544	0.9910
Ch-RL PO (E5)	0.0985	0.9608	0.9917	0.9902	0.0051	0.9372	–	–	–
Ch-RS PO (E6)	0.0125	0.9968	0.2255	0.9928	0.0006	0.9929	–	–	–

Zero-order rate = mg/min, first-order rate = mg/min, Higuchi rate = $mg/min^{1/2}$, Korsmeyer–Peppas rate = mg/min^n

prevent collision of drug molecules and the subsequent formation of nuclei which lead to the thermodynamic instability (54). However, sometimes, crystallization inhibitors can reduce the active ingredient diffusivity in the matrix, which could bring a reduction of drug release; this may be the case of NE type.

Release data of tramadol from Eudragit–chitosan mixed matrix films run as expected from release studies concerning single-polymer films (Table V). E4 was the slowest and E5 was the fastest. As RL contains more quaternary ammonium substitution, which makes it more hydrophilic, and water can penetrate more freely into RL than RS as previously noticed in swelling studies, therefore faster release was attained by E5 film. The release results run more or less in accordance with film thickness (Table II); as previously listed, the release rate is generally inversely related to film thickness (39,53).

Mixing of chitosan with Eudragit has almost accelerated the release of *T* from Eudragit films especially in the case of NE type. This may be due to physical links taking place between chitosan and Eudragit (as proved in IR study), allowing the liberation of free *T* from the polymeric matrix. The same amount of the same plasticizer (glycerin) was used for all of them; differences in drug release can be attributed to drug–polymer(s), polymer–polymer, and polymer–plasticizer interactions in addition to what is listed before concerning intrinsic polymer properties. The additional presence (compared to NE film) of a water-soluble plasticizer, glycerin, which can easily penetrate E4 film structure, renders the film more hydrophilic, favoring more water absorption into the polymer, which may have a positive impact on drug release. Another interpretation of the faster drug release from E4 than from NE film is that the addition of the plasticizer may therefore allow for easier drug diffusion (13). The observed release pattern showing a high release rate at the beginning which then monotonically decreased with time is a typical behavior for diffusion-controlled drug delivery system. With increasing time, the length of the diffusion pathway increases; thus, the concentration gradient which is the driving force for diffusion decreases and, consequently, the drug release rate decreases. This phenomenon can be well explained by Fick's second law of diffusion (55). The E4 release pattern seems to be the targeted one, achieving a combined rapid and prolonged drug release. Statistical analysis of different release parameters is listed in Table V.

Korsmeyer–Peppas mathematical model was only applicable in case of E4, and diffusion-controlled release can be detected (n=0.1544; Table VI). The Higuchian release rate was equal to 0.3678 mg/min$^{1/2}$; also, E5 followed Higuchi square root of time model, and the release rate was 0.9917 mg/min$^{1/2}$, while in the case of E6, zero order yielded best fitting.

Ex vivo permeation studies

The data, expressed as cumulative amount of drug permeated as a function of time (Fig. 4), were fitted to the equation of Fick's second law of diffusion (56). As most formulations attained almost complete drug permeation at 24 h, the cumulative amount of drug permeated % at 5 h (% Q_5) was calculated to compare between different formulae. Also, the steady-state flux (J), the lag time (T_l), the diffusion coefficient (D), the partition coefficient (K), the permeability coefficient (P), and the permeation efficiency (PE) were calculated (57,58).

In the current work, the thickness of the skin was found to be 300±50 μm.

It is actually difficult to precise the accurate diffusional path length (L) of a molecule through the skin due to tortuosity of the route and the repeated partitioning and diffusion across the structured bilayers of the skin; therefore, the diffusion and partition coefficients have been normalized. The partition parameter or normalized partition coefficient (K_{apparent}=KL) reflects the distribution of the drug between the skin and the donor phase, while the diffusion parameter or diffusivity or normalized diffusion coefficient ($D_{\text{apparent}}=D/L^2$) reflects the mobility of the drug in the skin (59). The permeability coefficient is equal to the product of KL and D/L^2.

Permeation data are listed in Tables VII and VIII. The data correlate with the *in vitro* release results. Chitosan film

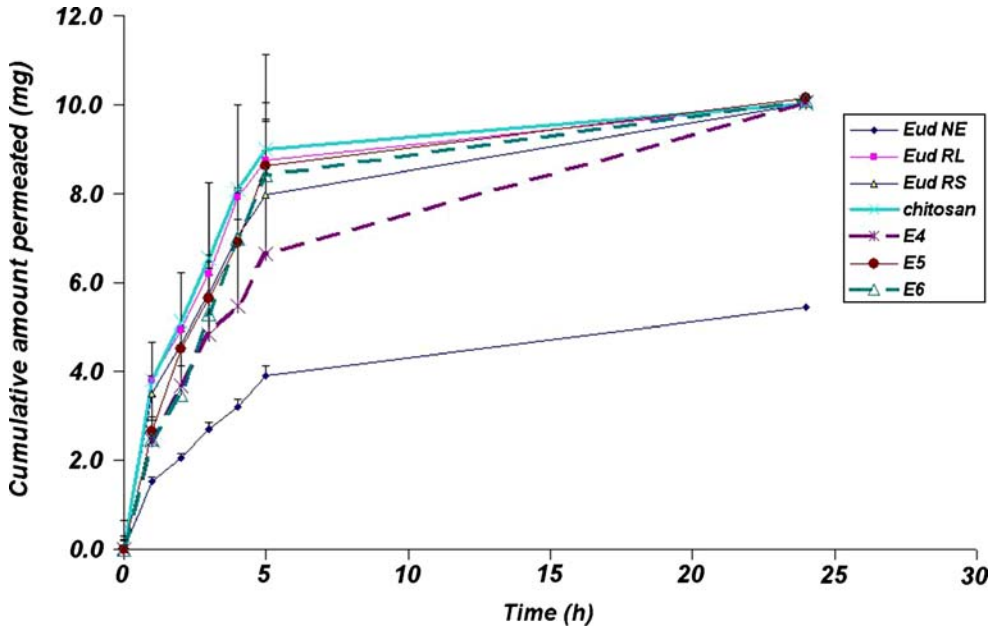

Fig. 4. Permeation profiles of tramadol HCl from monolithic matrix films

Table VII. Permeation of Tramadol HCL from the Monolithic Matrix Films

Time (min)	Cumulative amount released (mg)±SD						
	NE 30D	RL PO	RS PO	Chitosan	E4	E5	E6
1	1.54±0.07	3.82±0.12	3.50±0.16	3.80±0.64	2.46±0.31	2.66±0.19	2.48±0.22
2	2.05±0.09	4.93±0.15	4.62±0.21	5.11±0.87	3.68±0.99	4.51±0.32	3.48±0.43
3	2.72±0.12	6.19±0.19	5.77±0.26	6.53±1.11	4.84±1.30	5.64±0.40	5.30±0.65
4	3.20±0.14	7.90±0.25	7.05±0.32	8.08±1.71	5.46±1.62	6.90±0.98	6.99±0.86
5	3.90±0.17	8.73±0.27	7.97±0.37	8.99±1.91	6.63±1.97	8.61±1.22	8.43±1.04
24	5.42±0.23	10.04±0.31	10.03±0.46	10.03±2.13	10.05±2.99	10.14±1.43	10.09±1.24
Q_5 %	39.03±1.66[a]	87.31±2.72[b]	79.70±3.65[c]	89.93±19.08	66.27±19.68[d]	86.12±12.18[g]	84.27±10.37[i]
PE %	41.71±1.77[a]	85.63±2.68[b]	81.65±3.74[c]	86.97±18.18	74.24±21.77[d]	84.22±11.53[g]	82.64±10.13[j]
Flux (mg/cm^{2}h)	0.118±0.00[a]	0.256±0.01[b]	0.227±0.01[c]	0.267±0.07	0.202±0.08[e]	0.286±0.05[g]	0.308±0.04[i]
P (cm/h)	0.012±0.00[a]	0.026±0.00[b]	0.023±0.00[c]	0.027±0.01	0.020±0.01[d]	0.029±0.01[g]	0.031±0.00[i]
T_1 (h)	0.072[a]	0.022[c]	0.011[a]	0.030	0.074[f]	0.205[h]	0.356[k]
Diffusion coefficient $D\times10^{-4}$ (cm^2/h)	22.388[a]	68.182[c]	136.364[a]	50.000	20.270[e]	7.317[h]	4.213[k]
Partition coefficient K	0.158[b]	0.113[c]	0.050[a]	0.160	0.299[d]	1.172[h]	2.193[k]
D apparent (h^{-1})	2.488[a]	7.576[c]	15.152[a]	5.556	2.252[e]	0.813[h]	0.468[k]
K apparent (cm)	0.005[c]	0.003[c]	0.002[a]	0.004	0.009[d]	0.035[h]	0.066[k]

Each value represents the mean±SD (n=3)
[a] Significant difference (p<0.001) compared to chitosan
[b] Non-significant difference (p>0.05) compared to chitosan
[c] Significant difference (p<0.05) compared to chitosan
[d] Significant difference (p<0.001) compared to NE
[e] Significant difference (p<0.05) compared to NE
[f] Non-significant difference (p>0.05) compared to NE
[g] Non-significant difference (p<0.05) compared to RL
[h] Significant difference (p<0.001) compared to RL
[i] Significant difference (p<0.05) compared to RS
[j] Non-significant difference (p>0.05) compared to RS
[k] Significant difference (p<0.001) compared to RS

showed the most rapid drug skin permeation and followed zero-order kinetics showing a membrane-dependent permeation. The initial quick diffusion across the skin (burst effect) would be beneficial, as it would help achieve the therapeutic plasma concentration of the drug in minimum time and the constant permeation later on would then provide a sustained and controlled release of the drug. Burst effect might be due to initial migration of the drug towards the surface of the matrix and, hence, the surface of the skin and the high concentration gradient which is the main driving force.

As expected from release results and noticed from permeation data listed in Table VII, Eudragit® NE type showed the slowest drug permeation profile due to intrinsic properties in addition to the absence of plasticizer. PEG is a hydrophilic compound capable of increasing transdermal flux (60); however, its use as plasticizer for RL and RS films may be one of the reasons for the lower permeation noticed compared to chitosan film. Some previous studies have ranked the permeability enhancement effect of PEG 400 to be lower than some other plasticizers (22). Also, polymethacrylates can be used as antinucleating agents (54); however, sometimes, they can reduce the active ingredient diffusivity in the matrix, which could bring a decrease of the drug amount permeated through the skin; this may be the case of NE type. As expected, the permeation of tramadol from RL type was faster than from RS type. The amphiphilic properties of Eudragits may facilitate partitioning within different skin layers; this may be reflected in the relatively high values of D (Table VII). Diffusion through skin was the rate-determining step for the permeation of tramadol from Eudragit films; this was detected from the best fitting of the permeation data to zero-order kinetics (Table VIII).

The formation of IPN in mixed polymers system and the alteration of cross-linking between polymeric chains together with the modulation of structural and conformational arrangements of polymers provoke different release and permeation profiles.

Considering the permeation data and its statistical analysis listed in Table VII, it is obvious that E4 film showed a desired sustained, yet rapid enough, profile, while E5 and E6 showed an initial burst effect; the initial drug amount permeated % during the first 5 h was 66.27±19.68, 86.12±12.18, and 84.27±10.37, respectively. These results were expected from previous studies comprising water uptake capacity and drug release properties from single Eudragit

Table VIII. Permeation Kinetics of Tramadol HCL from Monolithic Matrix Films

Formula	Correlation coefficient		
	Zero order	Higuchi order	1st order
NE 30D film	0.9969	0.9779	0.9864
RL PO film	0.9910	0.9767	0.9823
RS PO film	0.9980	0.9881	0.9818
Chitosan	0.9946	0.9889	0.9745
E4	0.9899	0.9912	0.9519
E5	0.9930	0.9854	0.9507
E6	0.9932	0.9684	0.9819

films (NE, RL, or RS) or composite chitosan–Eudragit films. These prove the importance of preliminary swelling and release studies and showed that the first phenomena occurring after patch application on skin will have a profound impact on topical and systemic drug delivery.

It is noticed that E5 and E6 films permeation profiles showed a linear relationship during steady-state flux between the cumulative amount permeated and time demonstrating a zero-order permeation model. This clearly indicates a skin-dependent permeation which is strongly controlled by the stratum corneum diffusion process, while the permeation profile of E4 film showed the most linear relationship between the cumulative amount permeated and the square root of time (Table VIII), demonstrating a device-controlled transdermal delivery depending mainly on the system design rather than the skin barrier, which may allow for a more consistent and programmed drug delivery. In the case of E5 and E6 as well as chitosan film, the major resistance to tramadol transdermal delivery resides in the skin, more precisely, the stratum corneum; hence, the clinical performance may depend on the site of application as well as the system design. It is therefore necessary to properly determine the site of application to guarantee a uniform consistent drug delivery (61). These results also demonstrate the possibility of obtaining different drug delivery profiles and mechanisms by simply mixing different polymers together according to a preplanned system.

CONCLUSION

The inclusion of two polymers in the innovative films has resulted in particularly interesting findings because an appropriately high transdermal flux in the early times of patch application was obtained, suggesting a quick onset of the relevant plasma levels, followed by an extended release profile which can guarantee the long-lasting analgesia. Chitosan–Eudragit® NE 30D (1:1) mixed monolithic film attained the most desirable profile and compromised physicochemical properties as well. These encouraging preliminary results have generated an enthusiasm which pushed us to achieve further biological and pharmacological evaluations (which will be presented in a complementary research paper). The current study can have positive contribution in the world of pain fighting and management by offering an around-the-clock analgesia with the use of lesser medications together with a favorable safety profile.

REFERENCES

1. J. D. Schim, and P. Stang. Overview of pain management. *Pain. Practice*. **4**:S4–S18 (2004).
2. R. B. Raffa. Pharmacology of oral combination analgesics: rational therapy for pain. *J. Clin. Pharm. Ther*. **26**:57–264 (2001).
3. H. Malonne, M. Coffiner, D. Fontaine, B. Sonet, A. Sereno, and A. Peretz. Long-term tolerability of tramadol LP, a once-daily formulation, in patients with osteoarthritis or low back pain. *J. Clin. Pharm. Ther*. **30**:113–120 (2005).
4. L. J. Scott, and C. M. Perry. Tramadol, a review of its use in perioperative pain. *Drugs*. **60**(1):139–176 (2000).
5. B. R. Olin. Central analgesics. In M. R. Riley (ed.), *Drug Facts and Comparisons*, 54th ed., Wolters Kluwer, St. Louis, 2000, pp. 817–818.
6. P. J. Fudala, and R. E. Johnson. Development of opioid formulations with limited diversion and abuse potential. *Drug Alcohol Depend*. **83S**:S40–S47 (2006).
7. B. Thomas, and B. Finnin. The transdermal revolution. *Drug Disc. Today*. **9**(16):697–703 (2004).
8. C. R. Lee, M. D. Tavish, and E. M. Sorkin. Tramadol: a preliminary review. *Drugs*. **46**:313–340 (1993).
9. G. G. Cameron, and J. W. McGinity. Controlled release theophylline tablet formulations containing acrylic resins. *Drug Dev. Ind. Pharm*. **13**:1409–1427 (1987).
10. Z. Lu, W. Chen, and J. Hamman. Chitosan–polycarbophil complexes in swellable matrix systems for controlled drug release. *Curr. Drug Deliv*. **4**:257–263 (2007).
11. G. N. Kalinkova. Studies of beneficial interactions between active medicaments and excipients in pharmaceutical formulations. *Int. J. Pharm*. **187**:1–15 (1999).
12. S. Senel, G. Ikinci, S. Kas, A. Yousefi-Rad, M. F. Sargon, and A. A. Hincal. Chitosan films and hydrogels of chlorhexidine gluconate for oral mucosal delivery. *Int. J. Pharm*. **193**:197–203 (2000).
13. X. Zhang, Y. Wang, J. Wang, Y. Wang, and S. Li. Effect of pore former on the properties of casted film prepared from blends of Eudragit® NE 30 D and Eudragit® L 30 D-55. *Chem. Pharm. Bull*. **55**(8):1261–1263 (2007).
14. C. Amnuaikit, I. Ikeuchi, K. Ogawara, K. Higaki, and T. Kimura. Skin permeation of propranolol from polymeric film containing terpene enhancers for transdermal use. *Int. J. Pharm*. **289**:167–178 (2005).
15. S. B. Tiwari, T. K. Murthy, M. R. Pai, P. R. Mehta, and P. B. Chowdary. Controlled release formulation of tramadol hydrochloride using hydrophilic and hydrophobic matrix system. *AAPS PharmSciTech*. **4**(3):1–6 (2003).
16. B. Mukhejee, S. Mahapatra, R. Gupta, B. Patra, A. Tiwari, and P. Arora. A comparison between povidone–ethylcellulose and povidone–eudragit transdermal dexamethasone matrix patches based on *in vitro* skin permeation. *Eur. J. Pharm. Biopharm*. **59**:475–483 (2005).
17. S. Blanchon, G. Couarraze, F. Rieg-Falson, G. Cohen, and F. Puisieux. Permeability of progesterone and a synthetic progestin through methacrylic films. *Int. J. Pharm*. **72**:1–10 (1991).
18. F. Lecomte, J. Siepmann, M. Walther, R. J. MacRae, and R. Bodmeier. Polymer blends used for the aqueous coating of solid dosage forms: importance of the type of plasticizer. *J. Control. Release*. **99**:1–13 (2004).
19. C. Tas, Y. Ozkan, A. Savaser, and T. Baykara. *In vitro* release studies of chlorpheniramine maleate from gels prepared by different cellulose derivatives. *IL Farmaco*. **58**:605–611 (2003).
20. S. N. Murthy, S. R. R. Hiremath, and K. L. K. Paranjothy. Evaluation of carboxymethyl guar films for the formulation of transdermal therapeutic systems. *Int. J. Pharm*. **272**:11–18 (2004).
21. C. Padula, S. Nicoli, P. Colombo, and P. Santi. Single-layer transdermal film containing lidocaine: modulation of drug release. *Eur. J. Pharm. Biopharm*. **66**(3):422–428 (2007).
22. C. M. Heard, S. Johnson, G. Moss, and C. P. Thomas. *In vitro* transdermal delivery of caffeine, theobromine, theophylline and catechin from extract of Guarana, Paullinia Cupana. *Int. J. Pharm*. **317**(1):26–31 (2006).
23. R. Panchagula, R. Bokalial, P. Sharma, and S. Khandavilli. Transdermal delivery of naloxone: skin permeation, pharmacokinetic, irritancy and stability studies. *Int. J. Pharm*. **293**:213–223 (2005).
24. I. Z. Schroeder, P. Franke, U. F. Schaefer, and C. Lehr. Development and characterization of film forming polymeric solutions for skin drug delivery. *Eur. J. Pharm. Biopharm*. **65**:111–121 (2007).
25. M. E. Aulton, and M. H. Abdul-Razzak. The mechanical properties of hydroxypropylmethylcellulose films derived from aqueous systems, part 1: the influence of plasticizers. *Drug. Dev. Ind. Pharm*. **7**:649–668 (1981).
26. A. M. Wokovich, S. Prodduturi, W. H. Doub, A. S. Hussain, and L. F. Buhse. TDDS adhesion as a critical safety, efficacy and quality attribute. *Eur. J. Pharm. Biopharm*. **64**:1–8 (2006).
27. S. Wittaya-areekul, C. Prahsarn, and S. Sungthongjeen. Development and *in vitro* evaluation of chitosan–eudragit RS 30D composite wound dressings. *AAPS PharmSciTech*. **7**(1):Article30 (2006).
28. C. Reumnan-Lopez, and R. Bodmeier. Mechanical and water vapor transmission properties of polysaccharide films. *Drug. Dev. Ind. Pharm*. **22**:1201–1209 (1996).
29. J. Viyoch, T. Sudedmark, W. Srema, and W. Suwongkrua. Development of hydrogel patch for controlled release of alpha-hydroxy acid contained in tamarind fruit pulp extract. *Int. J. Cosmet. Sci*. **27**:89–99 (2005).

30. M. R. Harris, and I. Ghebre-Sellassie. Aqueous polymeric coating for modified release oral dosage forms. In J. W. McGinity (ed.), *Aqueous Polymeric Coatings for Pharmaceutical Dosage Forms, 2nd ed*, Marcel Dekker, New York, 1997, pp. 81–100.
31. Eudragit® Handbook. Rohm GmbH, Darmstadt, Germany, 1997.
32. J. Fang, Y. Huang, H. Lin, and Y. Tsai. Transdermal iontophoresis of sodium nonivamide acetate. IV. Effect of polymer formulations. *Int. J. Pharm*. **173**:127–140 (1998).
33. P. Rama Rao, and P. V. Diwan. Formulation and *in vitro* evaluation of polymeric films of diltiazem hydrochloride and indomethacin for transdermal administration. *Drug Dev. Ind. Pharm*. **24**:327–336 (1998).
34. A. D. Woolfson, D. F. McCafferty, and G. P. Moss. Development and characterization of a moisture-activated bioadhesive drug delivery system for a percutaneous local anesthesia. *Int. J. Pharm*. **169**:83–94 (1998).
35. A. Akhgari, F. Farahmand, A. Garekani, A. Sadeghi, and T. F. Vandamme. Permeability and swelling studies on free films containing inulin in combination with different polymethacrylates aimed for colonic drug delivery. *Eur. J. Pharm. Sci*. **28**:307–314 (2006).
36. J. Guo, G. W. Skinner, W. W. Harcum, and P. E. Barnum. Pharmaceutical applications of naturally occurring water-soluble polymers. *PharmSciTech Today*. **1**(6):254–261 (1998).
37. L. Perioli, V. Ambrogia, M. Riccia, S. Giovagnolia, M. Capuccellab, and C. Rossi. Development of mucoadhesive patches for buccal administration of ibuprofen. *J. Cont. Rel*. **99**:73–82 (2004).
38. S. Cafaggi, R. Leardi, B. Parodi, E. Caviglioli, E. Russo, and G. Bignardi. Preparation and evaluation of a chitosan salt–poloxamer 407 based matrix for buccal drug delivery. *J. Control. Release*. **102**:159–169 (2005).
39. P. Rama Rao, and P. V. Diwan. Permeability studies of cellulose acetate free films for transdermal use: influence of plasticizers. *Pharm. Acta Helv*. **72**:47–51 (1997).
40. J. Hadgraft. Skin, the final frontier. *Int. J. Pharm*. **224**:1–18 (2001).
41. E. Karavas, G. Ktistis, and E. Georgarakis. Miscibility behavior and formation mechanism of stabilized felodipine–polyvinylpyrrolidone amorphous solid dispersions. *Drug Dev. Ind. Pharm*. **31**:473–489 (2005).
42. A. L. Iordanskiia, M. M. Feldsteinb, J. Hadgraft, and N. A. Platea. Modeling of the drug delivery from a hydrophilic transdermal therapeutic system across polymer membrane. *Eur. J. Pharm Biopharm*. **49**:287–293 (2000).
43. Anon. TDDS—general release standards. *Pharmacopeial Forum*. **14**:3860–3865 (1980).
44. K. A. Khan. The concept of dissolution efficiency. *J. Pharm. Pharmacol*. **27**:48–49 (1975).
45. M. C. Gohel, and M. K. Panchal. Novel use of similarity factors f_2 and S_d for the development of diltiazem HCl modified-release tablets using a 3^2 factorial design. *Drug Dev. Ind. Pharm*. **28**:77–87 (2002).
46. N. Zaki, G. Awad, N. Mortada, and S. Abd El-Hady. Enhanced bioavailability of metoclopramide HCl by intranasal administration of a mucoadhesive *in situ* gel with modulated rheological and mucociliary transport properties. *Eur. J. Pharm. Sci*. **32**:296–307 (2007).
47. W. I. Higuchi. The analysis of data on the medicament release from ointments. *J. Pharm. Sci*. **51**:802–804 (1962).
48. R. W. Korsmeyer, R. Gurny, P. Buri, and N. A. Peppas. Mechanism of solute release from porous hydrophilic polymers. *Int. J. Pharm*. **15**:25–35 (1983).
49. N. A. Peppas. Analysis of Fickian and non-Fickian drug release from polymers. *Pharm. Acta Helv*. **60**:110–111 (1985).
50. T. Hayachi, H. Kanbe, M. Okada, M. Suzuki, and Y. Ikeda. Formulation study and drug release mechanism of a new theophylline sustained-release preparation. *Int. J. Pharm*. **304** (1–2):91–101 (2005).
51. J. E. Mockel, and C. Lippold. Zero-order drug release from hydrocolloid matrices. *Pharm. Res*. **10**:1066–1070 (1993).
52. K. G. Hollenbeck. In J. Swarbrick, and J. C. Boylan. Encyclopedia of pharmaceutical technology, vol 10. Dekker, New York, 1994, pp. 67–69.
53. M. Guyot, and F. Fawaz. Design and *in vitro* evaluation of adhesive matrix for transdermal delivery of propranolol. *Int. J. Pharm*. **204**:171–182 (2000).
54. F. Cilurzo, L. Tosi, S. Pagani, and L. Montanari. Polymethacrylates as crystallization inhibitors in monolayer transdermal patches containing ibuprofen. *Eur. J. Pharm. Biopharm*. **60**:61–66 (2005).
55. F. Siepmann, V. Le Brun, and J. Siepmann. Drugs acting as plasticizers in polymeric systems: a quantitative treatment. *J. Control. Release*. **115**:298–306 (2006).
56. K. Moser, K. Kriwet, Y. N. Kalia, and R. H. Guy. Passive skin permeation enhancement and its quantification *in vitro*. *Eur. J. Pharm. Biopharm*. **52**:103–112 (2001).
57. B. W. Barry. Dermatologic formulations: Percutaneous absorption, Marcel Dekker, New York, 1983.
58. G. L. Flynn, S. H. Yalkowsky, and T. J. Rosemann. Mass transport phenomena and models: theoretical concepts. *J. Pharm. Sci*. **63**:479–510 (1974).
59. P. Lim, X. Liu, L. Kang, P. Ho, Y. Chan, and S. Chan. Limonene GP1/PG organogel as a vehicle in transdermal delivery of haloperidol. *Int. J. Pharm*. **311**(1–2):157–164 (2006).
60. A. Casiraghi, F. Cilurzo, and L. Montanari. *In vitro* skin permeation of soy isoflavones. Communication 55, Symposuim Skin and Formulation. Paris, 2003.
61. K. Tojo, and T. Hikima. Bioequivalence of marketed transdermal delivery systems for tulobuterol. *Biol. Pharm. Bull*. **30**(8):1576–1579 (2007).